ANALYTICAL STUDY OF THE GENERATION AND CONTROL OF ORBIT ERRORS IN THE ANL 4-GEV CW ELECTRON MICROTRON DESIGN*

R. L. Kustom
Physics Division
Argonne National Laboratory
9700 S. Cass Avenue
Argonne, IL 60439

Summary

The 4 GeV CW Electron Microtron (GEM) Design has 3 linac sections and 3 dispersive straight sections. Six 60° sector bending magnets separate the linac and dispersion straight sections. A magnetic optical system has been designed within the dispersive straight sections to contain the beam during the 36 or 37 return passes through the linacs. A major concern is the effect of small alignment or field errors on the equilibrium or desired orbit with a relatively strong focussing system. The results of an analytical study which shows the effect of small random errors on the orbit are presented. A study was also undertaken on the control of the orbit position by making error measurements in one dispersive section and making an angular adjustment with a small dipole in the preceding dispersive section. The analysis indicates that the orbit position can be adequately and easily controlled in the presence of random alignment and field errors.

Introduction

ANL has completed a conceptual design for a 4 GeV CW electron microtron.[1] The design has three linac sections and three dispersive straight sections. Six 60° sector bending magnets separate the linac and dispersion straight sections. A magnetic optical system has been designed within the dispersive straight sections to contain the beam.[2] The long linac sections required for CW operation cause high sensitivity of the beam orbit to tolerance errors in the sector magnets and magnetic optical elements.

The present analysis shows that orbit displacements due to random errors can be kept within an acceptable level with a relatively simple feedback control system.

Algorithms for Calculating Equilibrium Orbit Displacements

The algorithms that "were" used for the analysis considered field errors, alignment errors in the transverse position at the entrance face, and rotation around the chord connecting the entrance and exit points of the bending magnets and errors in the focal length, alignment errors in the transverse position, and rotation around the center of the quadrupoles.

Figure 1 shows the location of the actual equilibrium orbit (EO) relative to the ideal EO in an unperturbed magnet and the ideal EO in a magnet frame that is translated by an amount Δx in the direction of the radius at the entrance face. Figure 2 shows the actual EO relative to the ideal EO and the ideal EO in a magnet frame that is rotated around the bisector of the chord connecting the entrance and exit points of the ideal EO. The

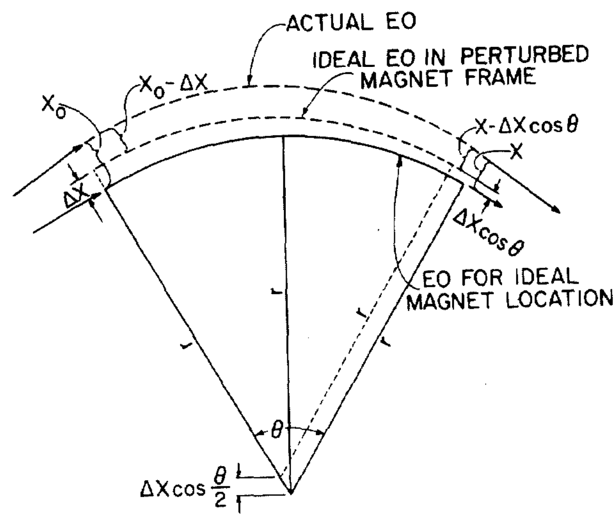

Fig. 1. Locations of actual and ideal EO in the sector bending magnets when the magnet is translated by Δx along the radius at the entrance to the magnet.

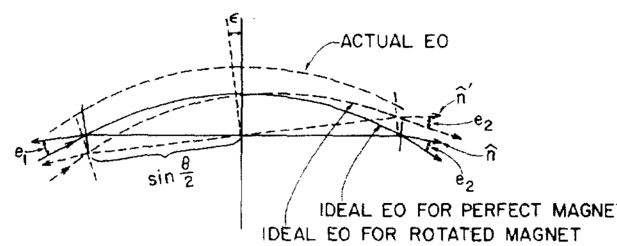

Fig. 2. Location of the actual EO and the ideal EO in the sector bending magnet when the magnet is rotated by ε around the center of the chord connecting the entrance and exit points of the ideal EO.

position and slope of the actual EO in the horizontal plane after exiting the magnet is given by

$$x = (x_o - \Delta x + \varepsilon r\sin\theta/2)(\cos\theta + \sin\theta\tan e_1) + r\sin\theta(x_o' - \varepsilon) + r(1-\cos\theta)(\Delta p/p - \Delta B/B) + \Delta x\cos\theta + \varepsilon r\sin\theta/2, \quad (1)$$

and

$$x' = (x_o - \Delta x + \varepsilon r\sin\theta/2)(1/r)\,[\tan e_2(\cos\theta + \sin\theta\tan e_1) + (\cos\theta\tan e_1 - \sin\theta)] + (x_o - \varepsilon)(\tan e_2\sin\theta + \cos\theta) + (\Delta p/p - \Delta B/B[\tan e_2(1-\cos\theta) + \sin\theta] + \varepsilon, \quad (2)$$

*Work supported by the U. S. Department of Energy under Contract W-31-109-Eng-38.

where x and x' are the differences in position and angular direction between the actual and ideal EO after exiting the sector bending magnet, x_o and x'_o are the differences in position and angular direction between the actual and ideal EO before entering the sector bending magnet, Δx is the displacement of the magnet in the direction of the radius, ε is the rotation around the center of the chord connecting the entrance and exit points of the ideal EO, θ is the bend angle in radians, r is the radius of curvature, e_1 and e_2 are the entrance and exit angles of the EO relative the normal to the magnet face, $\Delta p/p$ is the ratio of momentum error to the ideal momentum, and $\Delta B/B$ is the ratio of the field error to the ideal field.

Corrections for energy differences due to changes in path lengths in the bending magnet was incorporated in the program. The program could be started with any $\Delta p/p$ and an incremental length $(\delta\ell)_{new}$ was calculated from the existing incremental length, $(\delta\ell)_{old}$, by the following:

$$(\delta\ell)_{new} = (\delta\ell)_{old} + r(\pi/3 - \sin\pi/3)(\Delta p/p - \Delta B/B) \tag{3}$$

The momentum difference, $(\Delta p/p)_{new}$, was calculated after each pass through a linac using the equation;

$$(\Delta p/p)_{new} = (\Delta p/p)_{old} - \frac{\Delta E\omega\ \delta\ell\ \tan\phi_s}{90\ Br} \tag{4}$$

where ΔE is the energy gain per linac, ω is 2π × frequency, and θ_s is the phase stable angle of the linac.

The corresponding vertical displacement, y, and slope, y', after exiting the magnet relative to the vertical displacement, y_o, and slope, y'_o, before entering the magnet is given by

$$\begin{aligned} y = (y_o - \Delta y + \varepsilon r\sin\theta/2)(1 - \theta\tan e_1) \\ + (y'_o - \varepsilon)r\theta + \Delta y - \varepsilon r\sin\theta/2, \end{aligned} \tag{5}$$

$$\begin{aligned} y' = (y_o - \Delta y + \varepsilon r\sin\theta/2)(-1/r)(\tan e_1 + \tan e_2 \\ - \theta\tan e_1\tan e_2) + (y'_o - \varepsilon)(1 - \theta\tan e_2) + \varepsilon, \end{aligned} \tag{6}$$

where Δy is the displacement of the magnet and other parameters are the same as for equations (1) and (2).

The quadrupoles were treated as thin lenses in both horizontal and vertical planes, and the algorithms for both planes are identical; i.e.,

$$x = x_o + Lx'_o, \text{ and} \tag{7}$$

$$\begin{aligned} x' = (x_o/f)(1 - \Delta f/f) - (\Delta x/f)(1 - \Delta f/f) \\ + (\varepsilon L/2f)x'_o, \end{aligned}$$

where L is the length of the quadrupole, f is the focal length, Δf is the error in focal length, and the other parameters have the same definition as in equations (1) and (2).

Results of the Computer Calculations

The computer program calculated errors in the EO due to randomly generated alignment and field errors between the limits of $|\Delta B/B| < 0.0001$, $|\Delta x| < 0.0001$ m, and $|\varepsilon| < 0.0004$ radians for the sector bending magnets and $|\Delta f/f| < 0.001$,

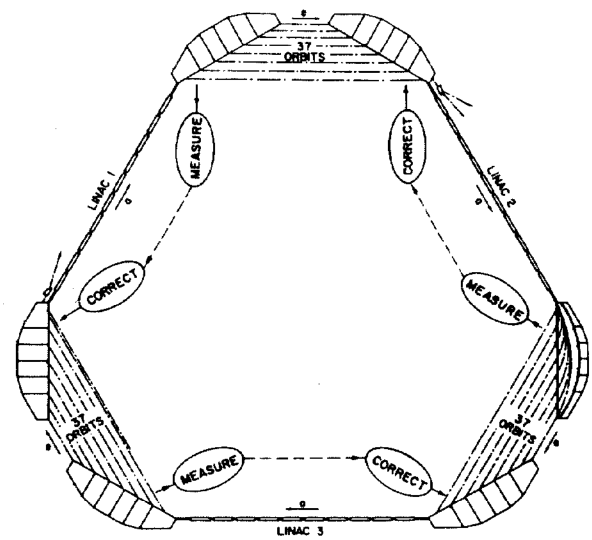

Fig. 3. Locations for equilibrium orbit error measurements and corrections.

$|\Delta x| < 0.0001$ m, and $|\varepsilon| < 0.0001$ radians for the qudrupoles. The magnitude of the errors were measured just after exiting a sector bending magnet into a dispersion region and minimized by adding an angular correction just before entering the previous sector bending magnet. This is schematically shown in Fig. 3.

Results of damping studies are shown in Figs. 4, 5, 6 and 7. Figures 4 and 5 show the damped orbits as dotted lines and the undamped orbits as solid lines. Figure 4 is for the horizontal plane and Fig. 5 is for the vertical plane. Each figure is for 3 full turns around the hexatron in the energy range of 220 to 535 MeV. Figure 6 shows the effect of different initial momentum errors of $\Delta p/p = 0.0$, $\Delta p/p = 0.0001$, and $\Delta p/p = 0.0001$. Figure 7 shows the effect of achieving measurement accuracies of 0.1, 0.2, and 0.3 mm at the points of measurement. Linac locations are indicated in Fig. 7 by the boxes drawn along the x-axis.

The magnetic fields in the correction magnets were less than 0.0135 T-m, which for a 3 cm long dipole is only 0.45 T.

As can be seen from Figs. 4 through 7, the undamped beam can grow to unacceptable displacements of 1 to 2 cm, but with damping can be controlled to within 2 or 3 mm and are kept to less than 1.5 mm in the linac regions. It's also apparent that no serious chromatic problems are generated by the damping system and that variations in measurement accuracy do not upset the operation of the damping system.

Computer runs with 3 times larger errors for $\Delta B/B$, Δx, and ε are shown for the 220 to 535 MeV horizontal orbits in Fig. 8. Even with the larger field and alignment errors, the displaced orbits in the linac only use about 50% of the available aperture. Although the complete parameter field has not been explored, it appears that the residual EO displacements are due mainly to the $\Delta B/B$ errors in sector magnets and that values near 4 to 5 × 10^{-4} can be tolerated and still get the beam through the linac apertures.

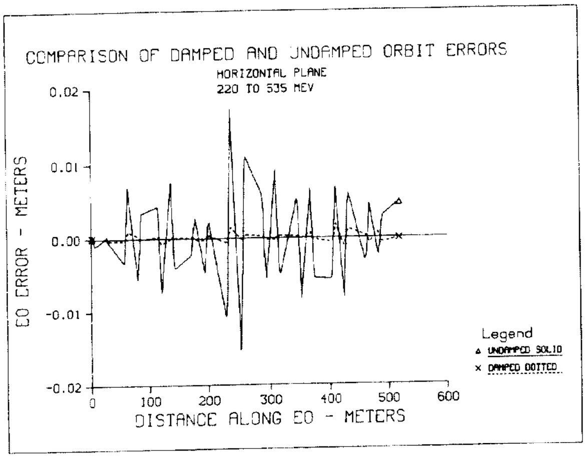

Fig. 4. Comparison of damped and undamped EO errors in the horizontal plane at energies between 220-535 MeV. Linac locations marked by boxes along the x-axis.

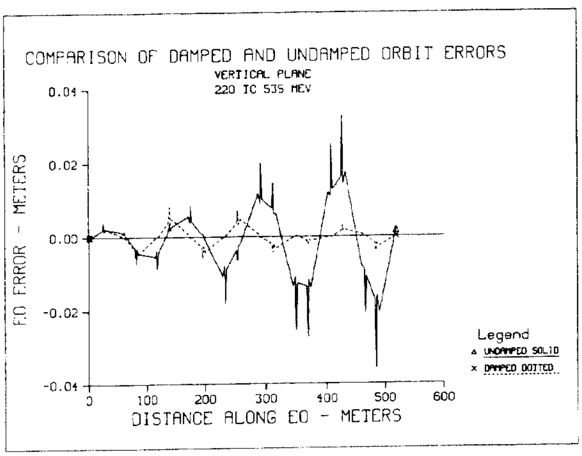

Fig. 5. Comparison of damped and undamped EO errors in the vertical plane at energies between 220-535 MeV. Linac locations marked by boxes along the x-axis.

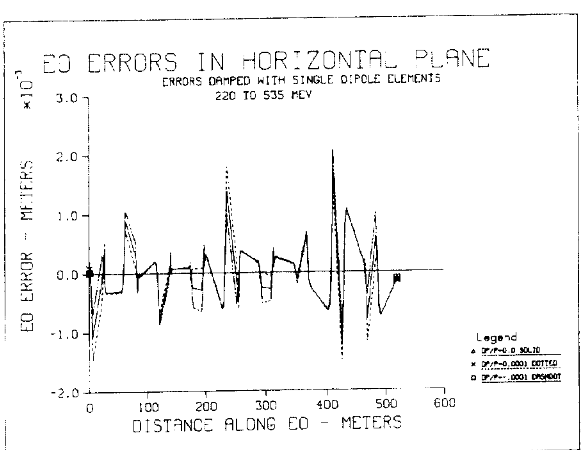

Fig. 6. Comparison of damped orbits in the horizontal plane for starting p/p of 0.0, +0.0001 and -0.0001 for energies between 220-535 MeV. Linac locations indicated by boxes on the x axis.

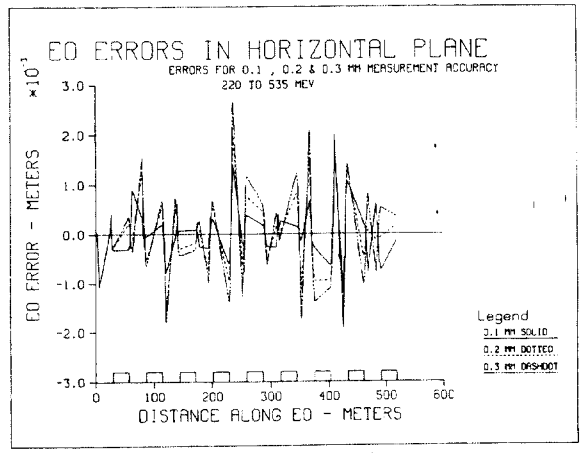

Fig. 7. Comparison of residual orbit errors after damping for measurement accuracies of 0.1, 0.2, and 0.3 mm.

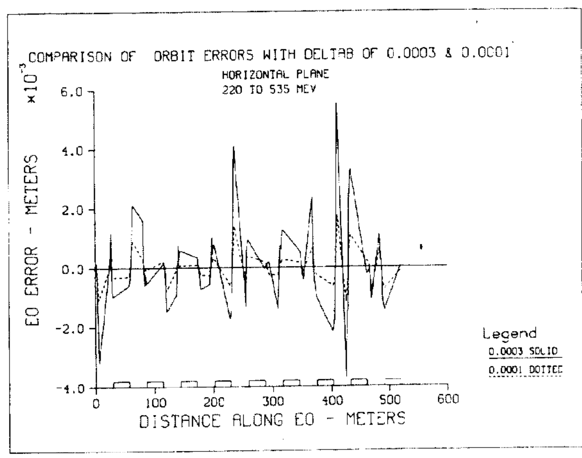

Fig. 8. Comparison of residual orbit errors after damping when the error in ∫Bdl of the sector bending magnets 0.0001 and 0.0003.

References

1. R. L. Kustom, GEM, ANL 4 GeV CW Electron Microtron Design, this conference.

2. E. Colton, Transverse Beam Containment in the ANL 4 GeV Microtron, this conference.